

Enthalpy, Volume, and Entropy Changes Associated with the Electron Transfer Reaction between the $^3\text{MLCT}$ State of $\text{Ru}(\text{Bpy})_3^{2+}$ and Methyl Viologen Cation in Aqueous Solutions

Claudio D. Borsarelli[†] and Silvia E. Braslavsky*

Max-Planck-Institut für Strahlenchemie, Postfach 10 13 65, D-45413 Mülheim an der Ruhr, Germany

Received: October 27, 1998; In Final Form: January 12, 1999

The electron-transfer reaction between the metal-to-ligand charge-transfer triplet ($^3\text{MLCT}$) state of $\text{Ru}(\text{bpy})_3^{2+}$ and the methyl viologen cation MV^{2+} was studied by laser-induced optoacoustic spectroscopy in the 8–35 °C temperature range in aqueous solutions in the absence and in the presence of various 0.1 M sodium salts. The enthalpy and the structural volume changes for the formation of the $^3\text{MLCT}$ state, $\Delta H_{\text{MLCT}} = (196 \pm 3)$ kJ/mol and $\Delta V_{\text{MLCT}} = (-3.6 \pm 0.2)$ cm³/mol, were independent of the presence of quencher or salt. The values of ΔH_{R} and ΔV_{R} for the production of the radical ion pair upon quenching of the $^3\text{MLCT}$ state by MV^{2+} strongly depended on the added salt. In neat water the expansion $\Delta V_{\text{R}} = (+10.1 \pm 1.2)$ cm³/mol is due to a decrease in solute–solvent interaction after electron transfer. This value can be calculated with the classical Drude–Nernst equation for electrostriction only if a semiempirical constant is employed instead of the theoretical one. The linear dependence between the relatively large changes in ΔH_{R} and ΔV_{R} along the series of added salts is explained in terms of enthalpy–entropy compensation effects due to the perturbation by the salts of the H-bond network in water. With the reported salt-independent reaction free energy a correlation between the reaction entropy and ΔV_{R} was found, i.e., $\Delta S_{\text{R}} = X/T \Delta V_{\text{R}}$, with $X = (14.4 \pm 0.8)$ kJ/cm³, similar to the $(c_p \rho / \beta)_T$ value at 303 K (near the isokinetic temperature, ca. 300 K) in aqueous solutions (c_p = heat capacity; ρ = mass density; β = volume expansion coefficient). The large values of the entropy term are due to the reorganization of the water network around the photoproduct radical ion pair, before recombination.

Introduction

Electron-transfer reactions in solution are accompanied by internal changes as well as by solvent rearrangements. Internal changes are the result of variations in bond lengths and angles, whereas solvent reorganization may be due to changes in the distribution of charges (electrostriction effect) and/or to changes in specific solute–solvent interactions concomitant with the electron-transfer reaction.

Laser-induced optoacoustic spectroscopy (LIOAS) is a suitable technique to study dynamic aspects of photoinduced chemical reactions, since the information obtained such as enthalpy and structural volume changes can be related to both internal and solvent rearrangements. LIOAS has been applied to the study of a few photoinduced intermolecular electron-transfer reactions such as the quenching of porphyrin triplets by quinones² as well as the quenching of the triplet metal-to-ligand charge transfer ($^3\text{MLCT}$) state of $\text{Ru}(\text{bpy})_3^{2+}$ by various Fe(III) salts.³ In the latter reaction, the structural volume changes strongly depended on the nature of the counterion of the iron salts, due to speciation effects. By using the LIOAS results together with the formation constants of the several iron complexes present before and after the reaction, we determined the partial molar volume at high dilution of various species, data not attainable by other methods.³

We recently found a linear correlation between the structural enthalpy (ΔH_{str}) and volume (ΔV_{str}) changes associated with

the formation of the $^3\text{MLCT}$ state of the complexes $\text{Ru}(\text{bpy})_2(\text{CN})_2$ and $\text{Ru}(\text{bpy})(\text{CN})_4^{2-}$ in aqueous solutions of 0.1 M monovalent salts.⁴ The ΔV_{str} values for these complexes were attributed to photoinduced changes in the hydrogen bond strength between the cyano ligands and the water molecules in the first solvation shell (specific solute–solvent interactions).⁵ Thus, the linear enthalpy–volume correlation in aqueous salt solutions was interpreted as arising from an enthalpy–entropy compensation effect induced by the added salt on the hydrogen bond network structure of water.⁴ Furthermore, the enthalpy–entropy compensation effect allowed us to determine the free energy for the formation of the $^3\text{MLCT}$ state of each complex and to find the correlation between the entropy change due to solvent changes and the structural volume change, i.e., $T\Delta S_{\text{str}} = (c_p \rho / \beta) \Delta V_{\text{str}}$ (c_p = heat capacity; ρ = mass density; β = volume expansion coefficient).

To further prove the thermodynamic basis of the structural volume changes in aqueous solutions, it is of interest to use a system in which no specific interactions (such as complex formation and/or hydrogen bonds) are present and analyze whether the changes observed can be explained by internal and/or solvent rearrangements. The oxidative quenching of the $^3\text{MLCT}$ state of $\text{Ru}(\text{bpy})_3^{2+}$ by the methyl viologen cation (MV^{2+}) appears to be a good system for this purpose, since, at least for the excited $\text{Ru}(\text{bpy})_3^{2+}$ complex, no specific interactions are expected in view of the hydrophobic nature of the ligands. We now report on the LIOAS study of this reaction in neat water and in aqueous solutions in the presence of various sodium salts.

We find again in the present case a linear correlation between the enthalpy and structural volume changes determined in the solutions of the various salts, associated with the production of

* To whom correspondence should be addressed. Silvia E. Braslavsky, Max-Planck-Institut für Strahlenchemie, D-45413 Mülheim an der Ruhr, Germany. Fax: +49 (208) 306 3681. E-mail: braslavskys@mpi-muelheim.mpg.de.

[†] Permanent address: Departamento de Química y Física, Universidad Nacional de Rio Cuarto, 5800 Rio Cuarto, Argentina.

the free radical ions upon quenching of the ${}^3\text{MLCT}$ state of $\text{Ru}(\text{bpy})_3^{2+}$ by MV^{2+} . The structural volume change is directly associated with the entropic term ($T\Delta S$) for the reaction. We further find that the solvent continuum model for electrostriction such as implied in the Drude–Nernst equation⁶ does not quantitatively explain the values determined for the structural volume changes, although qualitatively it describes the trend of the observed changes.

Experimental Section

Materials. $\text{Ru}(\text{bpy})_3\text{Cl}_2 \cdot 6\text{H}_2\text{O}$ ($\text{bpy} = 2,2'$ -bipyridine) and methyl viologen (MV^{2+}) dichloride hydrate were obtained from Aldrich and used as received. All the sodium salts were obtained from Merck or Fluka in the highest purity available and were dried under vacuum before use. Water was triply distilled.

In all cases the concentration of $\text{Ru}(\text{bpy})_3^{2+}$ was ca. 5×10^{-5} M. In neat water solutions, the LIOAS experiments were performed at several quencher concentrations, typically from 0 up to ca. 15 mM. For the experiments performed in the presence of 0.1 M sodium salts, the quencher concentration was fixed at 10 mM.

Methods. The principles of laser-induced optoacoustic spectroscopy (LIOAS) have been extensively described by Patel and Tam and by Tam.⁷ Several applications of LIOAS to chemical reactions have been reviewed by Braslavsky and Heibel.¹ Basically, the technique provides information on nonradiative deactivation pathways of excited states and/or transient species, such as triplets and radical ions. The experiment consists of measuring the pressure wave produced by the expansion of the compressible medium after pulse excitation. Two processes contribute to the volume changes in the solution: (i) a thermal term, ΔV_{th} , due to the heat released in internal conversion and/or intersystem crossing steps and (ii) a structural term, ΔV_{str} , related to chemical changes. In aqueous solutions, the separation of the heat and the structural volume changes contributions to the LIOAS signal is based on the concept that the heat released is translated into pressure through the thermoelastic parameters of the medium, i.e., the ratio $(c_p\rho/\beta)$ (where c_p is the heat capacity, ρ is the mass density, and β is the cubic expansion coefficient of the solvent), whereas the structural volume change is not translated through these parameters. In addition, the following assumptions are made: (a) the structural volume changes are invariant within the (relatively small) temperature range of the experiment and (b) the time behavior of the heat and structural volume changes is the same.

In time-resolved LIOAS, the sample signal is deconvoluted from that obtained upon irradiation of a solution with a reference compound, which releases as heat in few picoseconds all the absorbed photon energy.^{1,8} The deconvolution procedure yields the values of the preexponential term (φ_i) for each of the i th decays (normalized to that of the calorimetric reference) as well as the respective decay rate constant (k_i) which can be related to the elementary processes rate constants under consideration of the reaction mechanism. The following eq 1 is used in order to separate the above-mentioned contributions (i and ii) to φ_i .^{1,8}

$$E_\lambda \varphi_i = \Phi_{R,i} \Delta H_{R,i} + \Phi_{R,i} \Delta V_{R,i} \left(\frac{c_p \rho}{\beta} \right) = \Delta H_i + \Delta V_i \left(\frac{c_p \rho}{\beta} \right) \quad (1)$$

where E_λ is the excitation energy ($\cong 271.5$ kJ/mol at 441 nm) and $\Phi_{R,i}$, $\Delta H_{R,i}$, and $\Delta V_{R,i}$ are the quantum yield, the enthalpy, and the volume change per mole, respectively, associated with the i th process. The intercept and slope values of a linear regression of the plot of $E_\lambda \varphi_i$ vs $(c_p\rho/\beta)$ afford the total enthalpy

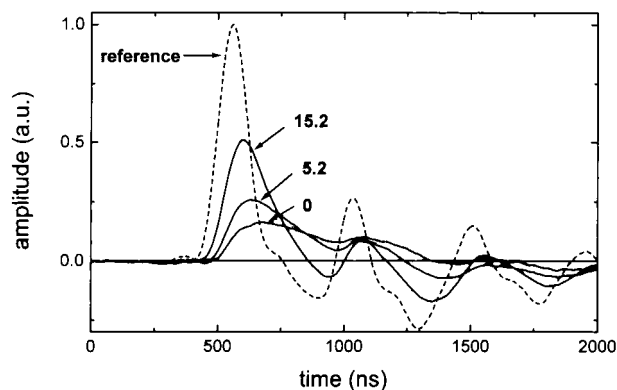


Figure 1. Reference-normalized LIOAS signals for $\text{Ru}(\text{bpy})_3^{2+}$ (solid lines) in water at 20 °C, as a function of MV^{2+} concentration (mM). All solutions were matched in absorbance at 441 nm ($A \approx 0.28$). The dash line is the signal for the calorimetric reference ($\text{Na}_2\text{Cr}_2\text{O}_7$).

change ΔH_i and the structural volume change ΔV_i associated with the i th step.

In aqueous media, the $(c_p\rho/\beta)$ ratio strongly depends on the temperature, due to the large temperature variation of β in water. This particular property allowed the application of eq 1 in a relatively narrow temperature range [8–35 °C (± 0.1)] which in turn permitted the assumption that, within the experimental error of 10%, no changes were produced in the kinetic parameters of the reaction.

The values of the $(c_p\rho/\beta)_T$ ratio in water at different temperatures were calculated by using the literature values of the individual parameters.^{9,10} In the case of 0.1 M salt solutions, the respective $(c_p\rho/\beta)_T$ ratios were determined by comparing the fluence-normalized LIOAS signal amplitude for a calorimetric reference in water with that in salt solutions, as was described previously.^{3,4}

In all cases, the LIOAS signals for the sample were fitted by deconvolution using a sum of two exponential-decay function and the Sound Analysis 3000 1.13 computational program (Quantum Northwest, Inc.). The signal of the calorimetric reference ($\text{Na}_2\text{Cr}_2\text{O}_7$) was used as the instrumental response.

Our LIOAS setup has been described in several publications.^{3,4,5,10} The excitation was a 15 ns (fwhm) laser pulse at 441 nm produced by an excimer laser (FL2000 Lambda Physik, XeCl)-pumped dye laser (EMG 101 MSC with the dye Coumarin 120, Lambda Physik). The laser beam width was shaped with a rectangular slit (0.2 \times 6) mm, so that the effective acoustic transient time in aqueous media was ca. 130 ns. This allowed resolution of lifetimes between ca. 20 and 1000 ns, by using the deconvolution procedure. A 40 μm poly(vinylidene fluoride) film was used as the pressure transducer. All solutions were deaerated by bubbling water-saturated Ar for 10–15 min.

The absorbances of reference and sample solutions were recorded with a Shimadzu UV-2102PC spectrophotometer and adjusted to the same value within 3% at 441 nm.

Quenching efficiencies η_q ($\pm 5\%$) were calculated as $\eta_q = (1 - \Phi_{\text{em}}/\Phi_{\text{em}}^0)$ by measuring the area under the emission spectrum of $\text{Ru}(\text{bpy})_3^{2+}$ with a Spex Fluorolog spectrofluorometer in the absence (Φ_{em}^0) and in the presence of various concentrations of MV^{2+} (Φ_{em}).

Results

Effect of quencher concentration. Figure 1 shows the reference-normalized LIOAS signals after excitation at 441 nm of aqueous solutions of $\text{Ru}(\text{bpy})_3^{2+}$ in the absence and in the presence of different concentrations of MV^{2+} . In all cases, the

TABLE 1: Quenching Efficiencies (η_q), Enthalpy (ΔH_1), and Structural Volume (ΔV_1) Changes and the Respective Lifetimes (τ_1), Associated with the Electron-Transfer Reaction from $^3[\text{Ru}^{\text{III}}(\text{bpy})_3]^{2+}$ to MV^{2+} in Neat Water. Temperature Range: 8–35 °C

[MV ²⁺] mM	η_q^a	ΔH_1 (kJ/mol)	ΔV_1 (cm ³ /mol)	τ_1 (ns)	ΔH_2 (kJ/mol)	ΔV_2 (cm ³ /mol)	τ_2^a (ns)
0	0	73 ± 5	-3.5 ± 0.2	<1	188 ± 6	3.7 ± 0.2	630 ± 5
2.8	0.32	78 ± 5	-3.4 ± 0.2	<1	160 ± 7	4.4 ± 0.2	442 ± 5
5.3	0.56	76 ± 5	-3.6 ± 0.2	<1	144 ± 8	4.8 ± 0.2	302 ± 5
10.0	0.76	75 ± 5	-3.6 ± 0.2	<1	134 ± 9	5.6 ± 0.3	156 ± 3
15.2	0.85	70 ± 5	-3.8 ± 0.2	<1	128 ± 9	5.9 ± 0.3	103 ± 3

^a Values at 20 °C.

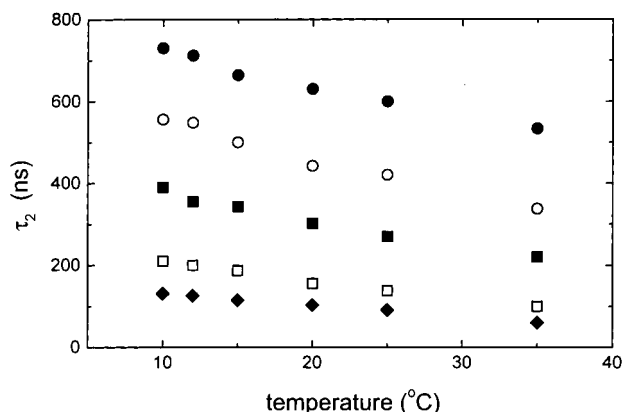


Figure 2. Temperature dependence of the lifetime, τ_2 , associated with the slow component of the LIOAS signals after excitation of Ru(bpy)₃²⁺ in water at several MV²⁺ concentrations: (●) 0 mM, (○) 2.8 mM, (■) 5.2 mM, (□) 10 mM, and (◆) 15.2 mM.

wave forms for the sample (solid lines) were time shifted with respect to the wave forms for the reference solution (dash line), which represents the temporal shape for an equivalent instantaneous reaction. Thus, after laser excitation, one or more reactions should take place within the time range analyzed with the LIOAS experiment (20–1000 ns). As the quencher concentration increased, the sample waveforms became larger in amplitude, while the time shift relative to the reference was smaller. These changes cannot be attributed to absorbance changes of the sample at the excitation wavelength, since the absorption spectrum above 360 nm remained constant upon addition of MV²⁺, as already reported in the literature.^{11,12}

The time evolution of the LIOAS signals was analyzed according to the deconvolution procedure described in the Experimental Section, by allowing a free fit of all parameters (two lifetimes and two preexponential factors). In every case the program found a fast decay ($\tau_1 < 1$ ns) with an amplitude, φ_1 , independent of the concentration of MV²⁺ and a second decay whose lifetime, τ_2 , was reduced upon increasing the MV²⁺ concentration and the temperature (Figure 2).

A typical example of deconvolution is shown in Figure 3. At temperatures lower than 15 °C, the sign of the first wave of the sample signal was negative, whereas for the reference it was positive. The latter sign was expected, since in water at $T > 4$ °C the cubic expansion coefficient is $\beta > 0$.¹ Furthermore, the first amplitude maxima for both sample and reference signals coincided in time. Therefore, the shape of the sample waveform at $T < 15$ °C indicates that a prompt contraction takes place. The contraction is then followed by an expansion. Regardless of the shape of the sample waveform, satisfactory fits of the LIOAS signals of the sample were obtained in all cases, as shown by the residuals distribution and the autocorrelation waveform in Figure 3.

The values of φ_i obtained at different temperatures for each process were plotted following eq 1. Typical plots are shown

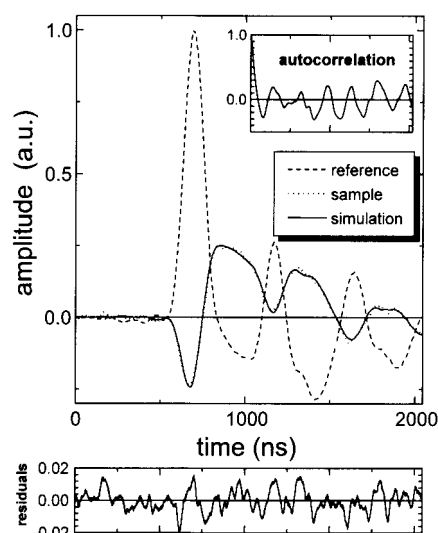


Figure 3. LIOAS signal for the sample and reference (Na₂Cr₂O₇) solutions after laser excitation at 441 nm of Ru(bpy)₃²⁺ in the presence of 2.8 mM MV²⁺ at 10 °C, together with the simulation curve, residuals distribution, and autocorrelation waveforms after fitting with a biexponential decay function; $\varphi_1 = -0.370$, $\tau_1 = 180$ ps; $\varphi_2 = 1.298$, $\tau_2 = 553$ ns, $\chi^2 = 4.21 \times 10^{-5}$. Note that the curves of sample and simulation essentially overlap.

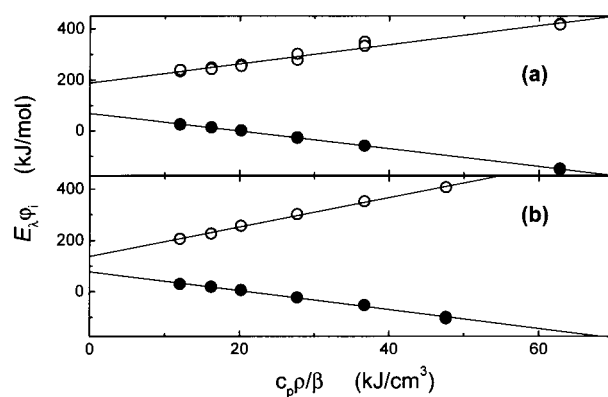


Figure 4. $E_x \varphi_1$ (full symbols) and $E_x \varphi_2$ (open symbol) values vs $(c_p \rho / \beta)$ (eq 1), for the LIOAS signals after excitation of Ru(bpy)₃²⁺ in (a) the absence and (b) the presence of 10.0 mM MV²⁺. The temperatures for the measurements were from left to right: 35, 25, 20, 15, 12, (b) 10, and (a) 8 °C.

in Figure 4 for excitation of Ru(bpy)₃²⁺ in the absence and in the presence of 10.0 mM MV²⁺. The intercepts (ΔH_i) and slopes (ΔV_i) values for all solutions are collected in Table 1.

The structural volume change associated with the formation of the ³MLCT state of Ru(bpy)₃²⁺, ΔV_{MLCT} , was obtained from the average of all ΔV_1 data in Tables 1 and 2, since ΔV_1 was independent of the presence of quencher and/or salt, and $\Phi_{\text{isc}} = 1$ (vide infra), i.e., $\Delta V_{\text{MLCT}} = \Delta V_1 / \Phi_{\text{isc}} = (-3.6 \pm 0.2)$ cm³/mol.

TABLE 2: Quenching Efficiencies (η_q), Enthalpy (ΔH_1), and Structural Volume (ΔV_1) Changes and the Respective Lifetimes (τ_1), Associated with the Electron-Transfer Reaction from $^3[\text{Ru}^{\text{III}}(\text{bpy})_3^{\bullet-}]^{2+}$ to MV^{2+} (10 mM) in 0.1 M Sodium Salt Aqueous Solutions. Temperature Range: 8–35 °C

salt solution	η_q^a	ΔH_1 (kJ/mol)	ΔV_1 (cm ³ /mol)	τ_1 (ns)	ΔH_2 (kJ/mol)	ΔV_2 (cm ³ /mol)	τ_2^a (ns)
NaF	0.84	78 ± 5	-3.8 ± 0.2	<1	76 ± 6	10.6 ± 0.5	102 ± 5
NaCl	0.88	72 ± 5	-3.6 ± 0.2	<1	192 ± 5	2.8 ± 0.2	78 ± 3
NaBr	0.89	77 ± 6	-3.6 ± 0.2	<1	197 ± 10	4.0 ± 0.3	69 ± 3
NaClO ₄	0.93	79 ± 6	-3.7 ± 0.3	<1	135 ± 7	7.2 ± 0.4	45 ± 3
NaH ₂ PO ₄	0.82	70 ± 6	-3.4 ± 0.3	<1	130 ± 7	6.5 ± 0.4	114 ± 5
NaAc	0.82	75 ± 9	-3.8 ± 0.5	<1	215 ± 15	1.5 ± 0.4	113 ± 5

^a Values at 20 °C, ±10%.

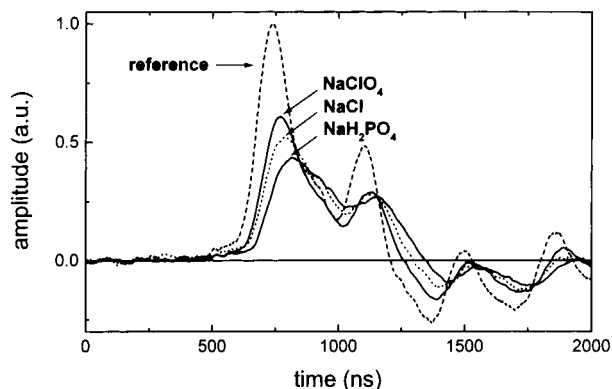


Figure 5. Reference-normalized LIOAS signals after excitation of $\text{Ru}(\text{bpy})_3^{2+}$ plus 10.0 mM MV^{2+} in aqueous solutions at 20 °C in the presence of several sodium salts. All the solutions were matched in absorbance at 441 nm ($A \approx 0.28$). The shape of the signal after excitation of the calorimetric reference ($\text{Na}_2\text{Cr}_2\text{O}_7$) solution (dash line) was independent of the presence of the various salts.

Effect of added salts. The quenching reaction was studied in 0.1 M solutions of various sodium salts. Figure 5 shows the reference-normalized signals for the sample ($\text{Ru}(\text{bpy})_3^{2+}$ + 10 mM MV^{2+}) in 0.1 M NaClO_4 , NaCl , and NaH_2PO_4 solutions at 20 °C. The signal shape was different for the different salts.

The signals were analyzed by using the same deconvolution procedure as in the case of neat water (see previous section). The amplitudes, φ_i , obtained at different temperatures for the fast ($\tau_1 < 1$ ns) and slow ($35 < \tau_2 < 180$ ns, depending on the salt and temperature) processes were plotted according to eq 1, yielding good linear plots (not shown). The respective intercepts (ΔH_i) and slopes (ΔV_i) values for the various salt solutions are presented in Table 2.

Discussion

I. The $^3\text{MLCT}$ State of $\text{Ru}(\text{bpy})_3^{2+}$. The enthalpy and structural volume changes associated with the instantaneous component of the LIOAS signals, ΔH_1 and ΔV_1 , are affected neither by the quencher concentration nor by the presence of salts (Tables 1 and 2). This confirms that these parameters correspond to the formation of the $^3\text{MLCT}$ state of $\text{Ru}(\text{bpy})_3^{2+}$, $^3[\text{Ru}^{\text{III}}(\text{bpy})_3^{\bullet-}]^{2+}$ (reaction A).³



The absorption band centered at 450 nm is the result of a $\text{Ru}(4d)-\text{bpy}(\pi^*)$ transition to $^1\text{MLCT}$.¹³ The emission is, however, from the $^3\text{MLCT}$ state, $^3[\text{Ru}^{\text{III}}(\text{bpy})_3^{\bullet-}]^{2+}$, formed with an intersystem crossing quantum yield of $\Phi_{\text{isc}} = 1$.¹⁴ Recently, a femtosecond study has confirmed that in acetonitrile solutions at room temperature the population of $^3[\text{Ru}^{\text{III}}(\text{bpy})_3^{\bullet-}]^{2+}$ is complete in ca. 0.3 ps.¹⁵ Then, the prompt component in the

LIOAS signal and its corresponding ΔH_1 and ΔV_1 values should be assigned to the formation of $^3[\text{Ru}^{\text{III}}(\text{bpy})_3^{\bullet-}]^{2+}$, as already stated in previous publications.^{4,5} This is further supported by the salt-independent values of ΔH_1 and ΔV_1 after excitation of $\text{Ru}(\text{bpy})_3^{2+}$ in solutions of various monovalent salts.⁴

In the absence of quencher, the slow component of the LIOAS signal is due to the relaxation of the $^3\text{MLCT}$ state of $\text{Ru}(\text{bpy})_3^{2+}$ to the ground state and $\Delta V_1 \approx -\Delta V_2$ (Table 1) also in agreement with previous studies.^{4,5} The lifetimes of the slow component τ_2 (full circles, Figure 2) agree well with the luminescence lifetimes of $^3[\text{Ru}^{\text{III}}(\text{bpy})_3^{\bullet-}]^{2+}$ in water in the same temperature range.^{16,17}

Taking into account that the partial molar volume of $\text{Ru}(\text{bpy})_3^{2+}$ at infinite dilution is $V^0 = (366 \pm 2)$ cm³/mol,¹⁸ the observed $\Delta V_{\text{MLCT}} = (-3.6 \pm 0.2)$ cm³/mol (Table 1) corresponds only to 1% of V^0 , underscoring the high sensitivity of LIOAS. This volume reduction of the excited state relative to the ground state has been assigned to a small shortening (ca. 0.01 Å) of the $\text{Ru}-\text{bpy}$ bonds, after the photoinduced intramolecular electron transfer from the central metal to the bpy ligand.¹⁹ Thus, $\text{Ru}(\text{bpy})_3^{2+}$ and its $^3\text{MLCT}$ state have essentially the same effective radius.

However, the “localized” charge transfer state $^*[(\text{bpy})_2\text{Ru}^{\text{III}}(\text{bpy}^{\bullet-})]^{2+}$ produced upon photoexcitation involves a strong increment of the dipole moment of the molecule, since the ground state of $\text{Ru}(\text{bpy})_3^{2+}$ has D_3 symmetry and no permanent dipole moment,^{13,20} whereas the dipole moment induced in the excited state is $\mu \cong (14 \pm 6)$ D.²¹ The question is then whether the electrical field associated with the dipole moment in the excited-state exerts an electrostrictive force on the solvation water molecules that could explain the structural volume change observed.

For the calculation of the electrostrictive volume change ΔV_{el} , it is possible to use a modification of the Drude–Nernst equation,⁶ eq 2,²² essentially applicable when there is no total charge separation and the dipole moment change is known,

$$\Delta V_{\text{el}} = -3N_a \frac{\Delta\mu^2}{r^3} \left(\frac{\partial\epsilon}{\partial P} \right)_T \frac{1}{2\epsilon + 1} \quad (2)$$

where N_a is Avogadro’s number, $\Delta\mu$ is the dipole moment change of the species, r is the effective cavity radius, and $(\partial\epsilon/\partial P)_T$ is the pressure dependence of the dielectric constant at constant temperature. Equation 2 yields a value $\Delta V_{\text{el}} \cong -0.4$ cm³/mol for the excitation of $\text{Ru}(\text{bpy})_3^{2+}$ in water, with $r = 4.8$ Å,¹⁸ $\Delta\mu = 14$ D,²¹ and $\partial\epsilon/\partial P = 3.68 \times 10^{-3}$ bar⁻¹ at 25 °C.²³ This value is ca. 10 times smaller than the experimental ΔV_{MLCT} , indicating already that the contraction upon $^3\text{MLCT}$ formation in water is mainly due to internal rearrangements and that electrostriction effects can be neglected, as it was postulated.¹⁹

Equation 2 is based on a dielectric continuum model and does not take into account any specific solute–solvent or solvent–

solvent interactions (such as hydrogen bonds). Nevertheless, for Ru(bpy)₃²⁺ in water, the application of eq 2 can be considered roughly valid due to the lack of hydrogen bridges or other donor–acceptor interactions between the bpy ligands and the water molecules.^{4,5} Thus, after the photoinduced dipole moment change, no important movements on the solvation water molecules are produced.

The average value $\Delta H_1 = (75 \pm 3)$ kJ/mol (Tables 1 and 2) represents the heat released upon deactivation of the excited singlet to ³[Ru^{III}(bpy)₃•⁻]²⁺, occurring in the picosecond time scale (see above). Then, the enthalpy content of the ³MLCT state relative to the ground state is calculated with eq 3

$$\Delta H_{\text{MLCT}} = \frac{E_\lambda - \Delta H_1}{\Phi_{\text{isc}}} \quad (3)$$

which yields $\Delta H_{\text{MLCT}} = (197 \pm 3)$ kJ/mol. A similar number, i.e., $\Delta H_{\text{MLCT}} = (196 \pm 6)$ kJ/mol is obtained considering the heat released in the decay of ³[Ru^{III}(bpy)₃•⁻]²⁺ in the absence of MV²⁺ (ΔH_2) plus the energy lost by emission ($\Phi_{\text{em}}E_{\text{em}}$) (eq 4)

$$\Delta H_{\text{MLCT}} = \frac{\Delta H_2 + \Phi_{\text{em}}E_{\text{em}}}{\Phi_{\text{isc}}} \quad (4)$$

$\Phi_{\text{em}}E_{\text{em}}$ is ca. 8 kJ/mol taking into account the Φ_{em} and E_{em} values for Ru(bpy)₃²⁺ in water.¹³

From the difference in the ground- and excited-state redox potentials in water, the free energy for the formation of ³[Ru^{III}(bpy)₃•⁻]²⁺ has been calculated to be $\Delta G_{\text{MLCT}} = 202.4$ kJ/mol.²⁴ A straightforward combination of the ΔH_{MLCT} and ΔG_{MLCT} values readily permits the calculation of a small entropy reduction for the formation of ³[Ru^{III}(bpy)₃•⁻]²⁺ in water, i.e., $\Delta H_{\text{MLCT}} - \Delta G_{\text{MLCT}} = T\Delta S_{\text{MLCT}} \approx -6$ kJ/mol. Although this value is within the error limits of each of the terms, a similar conclusion was extracted previously from spectroscopic studies.²⁵ Notwithstanding the error, at least qualitatively, this entropy correlates with the contraction observed by LIOAS, $\Delta V_{\text{MLCT}} = (-3.6 \pm 0.2)$ cm³/mol, assigned to internal changes in the molecular bonds upon excitation. In other words, ΔV_{MLCT} has the same sign as ΔS_{MLCT} .

II. Quenching Reaction of the ³MLCT State of Ru(bpy)₃²⁺ by MV²⁺. The temporal shape of the LIOAS signals was influenced by both the quencher concentration and the presence of salts (Figures 1 and 5). This behavior is the normal transducer response when the lifetime of the transient falls within the pressure integration time.^{8,26}

In every case, the lifetime of the slow LIOAS component τ_2 decreased upon increasing the quenching efficiency η_q (Tables 1 and 2). The η_q values calculated from the emission spectra after excitation of Ru(bpy)₃²⁺ (see the Experimental Section), or by using the decay lifetime τ_2 (determined by LIOAS) in the absence and in the presence of quencher, were in good agreement with those calculated with eq 5 and the reported quenching rate constant, k_q (5×10^8 M⁻¹ s⁻¹ for 10 mM MV²⁺)¹¹ under the same conditions.¹²

$$\eta_q = \frac{k_q \tau^0 [\text{MV}^{2+}]}{1 + k_q \tau^0 [\text{MV}^{2+}]} \quad (5)$$

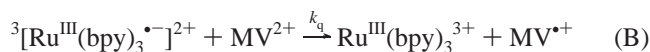
where τ^0 is the decay lifetime of ³[Ru^{III}(bpy)₃•⁻]²⁺ in the absence of quencher. Therefore, the decrease in the lifetime of the slow component in the LIOAS signal in the presence of MV²⁺ is

TABLE 3: Reaction Efficiency (η_R), Structural Enthalpy (ΔH_R), and Volume Changes (ΔV_R) Associated with the Formation of the Free Radical Ions Ru(bpy)₃³⁺ and MV•⁺ in Water. Temperature Range: 8–35 °C

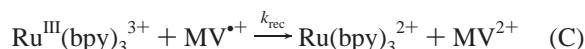
[MV ²⁺] mM	η_R^a	ΔH_R (kJ/mol)	ΔV_R (mL/mol)
2.8	0.08	351 ± 50	11.2 ± 1.2
5.2	0.14	343 ± 30	8.6 ± 1.5
10.0	0.19	319 ± 20	10.5 ± 1.4
15.2	0.21	340 ± 20	9.9 ± 1.5

^a Equation 6, error: ±10%.

assigned to the oxidative quenching of ³[Ru^{III}(bpy)₃•⁻]²⁺ by MV²⁺ (reaction B)^{11,12,24}



In aqueous media, the reaction B is near diffusionally controlled, with an exergonic driving force $\Delta G = (-40.5 \pm 1.9)$ kJ/mol, constant in several salt solutions.¹² With $\Delta G_{\text{MLCT}} = 202.4$ kJ/mol (see previous section), the free energy for the formation of the free radical ions from the parent compounds is calculated as ΔG_R ca. 162 kJ/mol. This difference provides the driving force for the back electron-transfer reaction C



Under the present experimental conditions, the bimolecular reaction C takes place well in the submillisecond time range,^{11,12} exceeding by far the upper time limit of the LIOAS experiment (ca. 5 μ s). This means that Ru^{III}(bpy)₃³⁺ and MV•⁺ are the final products in our observation time window. This was also confirmed when the fitting of the LIOAS signals was performed by adding a third component with a lifetime fixed between 1 and 5 μ s. In all cases the respective amplitude was very large (>10), indicating that permanent products (Ru^{III}(bpy)₃³⁺ and MV•⁺) storing part of the energy remained in the solution.

The increment in quencher concentration reduced ΔH_2 , whereas it increased ΔV_2 (Table 1). In the absence of added salts, these changes are related to the increment of the total efficiency of reaction B, η_R , which may be expressed as a product of three terms (eq 6)

$$\eta_R = \Phi_{\text{isc}} \eta_q \eta_{\text{esc}} \quad (6)$$

where η_q is the quenching efficiency (see eq 5) and η_{esc} refers to the probability of escape of the redox products from the solvent cage. In water, $\eta_{\text{esc}} = 0.25 \pm 0.05$, calculated taking into account the values reported by several authors.^{11,12,27–29} Under our experimental conditions, for MV²⁺ concentrations in the range 0–15.2 mM, we calculate that $0 \leq \eta_R \leq 0.21$ (Table 3).

The variation of the ΔV_2 and ΔH_2 values in 0.1 M solutions of various salts is rather complex (Table 2) although the quencher concentration was always the same (10 mM) and the quenching efficiencies were kept constant (± 10%).

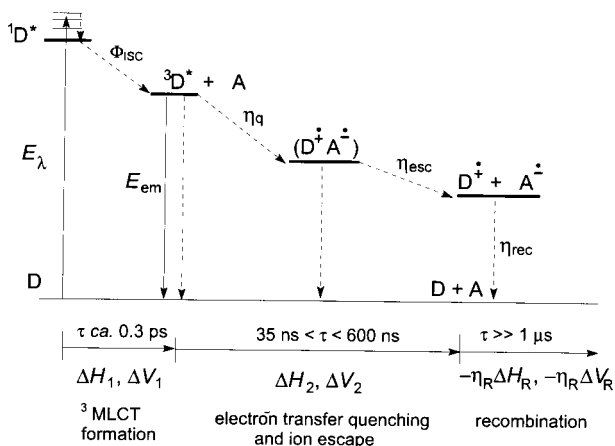
It is well-known that the presence of inert electrolytes, such as the current sodium salts, alters the kinetic parameters of reactions B and C.^{12,27–29} By using the recently reported η_{esc} values for reaction B as a function of temperature and salts,³⁰ the calculated (eq 6) extreme η_R values in the salt series are 0.08 and 0.14 for NaClO₄ and NaH₂PO₄, respectively (Table 2). However, between both support salts solutions the variation of ΔV_2 and ΔH_2 is not significant (Table 4). This means that the changes in η_R alone cannot responsible for the salt-induced variation in ΔV_2 and ΔH_2 . Furthermore, even in the presence

TABLE 4: Reaction Efficiency (η_R), Structural Enthalpy (ΔH_R), and Volume Changes (ΔV_R) Associated with the Formation of the Free Radical Ions $\text{Ru}(\text{bpy})_3^{3+}$ and 10 mM MV^{+} in 0.1 M NaX Aqueous Solutions

salt	η_R^a	ΔH_R (kJ/mol)	ΔV_R (mL/mol)
NaF	0.13	922 ± 72	54.0 ± 3.7
NaCl	0.13	50 ± 50	-6.1 ± 3.3
NaBr	0.12	-29 ± 44	3.5 ± 2.4
NaClO_4	0.08	680 ± 73	41.8 ± 3.9
NaH_2PO_4	0.14	503 ± 39	22.2 ± 2.5
NaAc	0.13	-153 ± 100	-17.5 ± 5.4

^a Equation 6, error: $\pm 10\%$.

SCHEME 1: Schematic Representation of the Photophysical Processes Taking Place during the Formation of the $^3\text{MLCT}$ State of $\text{Ru}(\text{bpy})_3^{2+}$ ($^3[\text{Ru}^{\text{III}}(\text{bpy})_3]^{2+}$, (Reaction A), and the Electron-transfer Quenching by MV^{2+} Producing Radical Ions (Reaction B). See Text. The Enthalpy and Structural Volumes Changes Associated with Each Process Are Indicated. Full Arrows Represent Optical Transitions and Dashed Arrows Represent Processes Releasing Heat. $D = \text{Ru}(\text{bpy})_3^{2+}$, $A = \text{MV}^{2+}$



of salts (which accelerates the recombination rate), the time range for the bimolecular reaction C exceeds well our upper time limit.²⁹ Thus, the charge recombination process can also be neglected.

III. Structural Enthalpy and Volume Changes of $\text{Ru}^{\text{III}}(\text{bpy})_3^{3+}$ and MV^{+} . Scheme 1 takes into account reactions A and B together, since they represent the global reaction in our time scale.

The structural enthalpy and volume changes per mole (relative to the ground state) associated with the formation of the free radical ions $\text{Ru}^{\text{III}}(\text{bpy})_3^{3+}$ and MV^{+} are calculated with eqs 7 and 8

$$\Delta H_R = \frac{E_\lambda - \Delta H_1 - \Delta H_2 - (1 - \eta_q)E_{\text{em}}\Phi_{\text{em}}}{\eta_R} \quad (7)$$

$$\Delta V_R = \frac{\Delta V_1 + \Delta V_2}{\eta_R} \quad (8)$$

The term $(1 - \eta_q)\Phi_{\text{em}}E_{\text{em}}$ in eq 7 represents the energy lost by emission by the fraction of nonquenched $^3[\text{Ru}^{\text{III}}(\text{bpy})_3]^{2+}$ species. In the absence of quencher, the values of both Φ_{em} and E_{em} were the same in the absence and in the presence of the salts. The calculated values of ΔH_R and ΔV_R are presented in Tables 3 and 4.

In the absence of added salts, the ΔH_R and ΔV_R values were independent of the quencher concentration, within the experimental error (Table 3), indicating the absence of specific solute–solute interactions in the quencher concentration range studied. The respective average values are $\Delta H_R = (338 \pm 20) \text{ kJ/mol}$ and $\Delta V_R = (+10.1 \pm 1.2) \text{ cm}^3/\text{mol}$.

The formation of the solvated free $\text{Ru}^{\text{III}}(\text{bpy})_3^{3+}$ and MV^{+} ions is thus accompanied by a global expansion, relative to the ground state ($\Delta V_R > 0$, Table 3). In turn, ΔV_R can be expressed as the sum of the partial molar volumes changes produced for each redox couple, i.e., $\text{Ru}(\text{bpy})_3^{3+/2+}$ and $\text{MV}^{+/2+}$ (eq 9).

$$V_R = (V_{\text{Ru}^{3+}}^o - V_{\text{Ru}^{2+}}^o) + (V_{\text{MV}^{+}}^o - V_{\text{MV}^{2+}}^o) = V_{\text{D}^{+}/\text{D}}^o + V_{\text{A}^{-}/\text{A}}^o \quad (9)$$

Recently, we reported that the structural volume change associated with the $\text{Ru}(\text{bpy})_3^{2+/3+}$ oxidation is $(-15.4 \pm 1.5) \text{ cm}^3/\text{mol}$, as determined by LIOAS following the quenching of the $^3\text{MLCT}$ state of $\text{Ru}(\text{bpy})_3^{2+}$ by $\text{Fe}(\text{aq})^{3+}$ in aqueous solutions.³ Using this value and the present ΔV_R , eq 9 yields the structural volume change contribution associated with the $\text{MV}^{2+/+}$ reduction, $\Delta V_{\text{A}^{-}/\text{A}}^o = (+25.5 \pm 2.7) \text{ cm}^3/\text{mol}$.

In a first approximation, both $\Delta V_{\text{D}^{+}/\text{D}}^o$ and $\Delta V_{\text{A}^{-}/\text{A}}^o$ can be considered as a sum of intrinsic and solvation contributions (eq 10),

$$\Delta V_i^o = \Delta V_{i,\text{int}}^o + \Delta V_{i,\text{sol}}^o \quad (10)$$

The intrinsic component results from changes in bond lengths and angles during the formation of the products. The solvation term represents all the changes produced in the solvent by changes in polarity, electrostriction, and dipole interactions during the reaction.

Complex ions of charges +2 and +3 with metal-to-ligand distances ranging from 2.0 to 2.4 Å, such as $\text{Ru}(\text{bpy})_3^{2+}$, may be considered as incompressible spheres, due to their very low calculated compressibility values.³¹ It has been suggested that $\text{Ru}(\text{bpy})_3^{2+}$ and its oxidized and reduced forms, $\text{Ru}(\text{bpy})_3^{3+}$ and $\text{Ru}(\text{bpy})_3^{+}$, have a similar size.³² Thus, for the oxidation process $\text{Ru}^{\text{II}}(\text{bpy})_3^{2+}$ to $\text{Ru}^{\text{III}}(\text{bpy})_3^{3+}$, $\Delta V_{\text{D}^{+}/\text{D},\text{int}}$ ca. 0. A similar assumption can be made for the reduction of MV^{2+} to MV^{+} , since the transferred electron is located in a π^* orbital of one of the pyridinium rings.³³

On the above basis, we consider that the principal contribution to the structural volume changes should originate in solvation effects. In the present case, the electron-transfer reaction occurs between ionic species with different sizes. This process produces a change in the magnitude of the electrostriction effect generated by the electrical field of each ion, although the number of charges is constant.

Taking into account that we are in the presence of a photoinduced charge change in the solvated ions, and to calculate the electrostriction effect, we apply the equation as originally proposed by Drude and Nernst.⁶ This equation describes the contraction of the solvent molecules with a homogeneous dielectric constant ϵ , due to the electrical field of an ion of charge z and radius r (eq 11)

$$\Delta V_{\text{el}} = -N_a \frac{z^2 e^2}{2r\epsilon^2} \left(\frac{\partial \epsilon}{\partial P} \right)_T = -B \frac{z^2}{r} \quad (11)$$

B is a reduced constant with a calculated value in water of 4.175 for the radius expressed in angstroms and the ion charge z as an integer number.³⁴ Thus, both $\Delta V_{\text{D}^{+}/\text{D}}^o$ and $\Delta V_{\text{A}^{-}/\text{A}}^o$ are

estimated by using eq 11, transferred into eqs 12 and 13 by considering that $r_{D^+} = r_D$ and $r_{A^-} = r_A$ (no internal changes):

$$\Delta V_{D^+/D}^o = -\frac{B}{r_D}(z_{D^+}^2 - z_D^2) = -\frac{B}{r_D}5 \quad (12)$$

$$\Delta V_{A^-/A}^o = -\frac{B}{r_A}(z_{A^-}^2 - z_A^2) = +\frac{B}{r_A}3 \quad (13)$$

The calculated values display the same qualitative tendency as the experimental structural volume changes (Table 4). In the Ru(bpy)₃^{2+/3+} oxidation process an increment on the electrostriction effect (contraction of the solvent) is expected due to the charge increment on the metal complex, whereas the opposite effect (less electrostriction, i.e., an expansion of the solvent) is predicted in the MV^{2+/+} reduction process, since the number of charges is decreased.

However, by using the calculated value of the constant B ($= 4.175 \text{ \AA}^{-1}$) for water at 25 °C, and the reported radii of 4.8 Å for Ru(bpy)₃²⁺,¹⁸ and 3.3 Å for MV²⁺,¹² eqs 12 and 13 afford $\Delta V_{D^+/D}^o = -4.3 \text{ cm}^3/\text{mol}$ and $\Delta V_{A^-/A}^o = +3.8 \text{ cm}^3/\text{mol}$, both values smaller than those derived from the LIOAS data (Table 3). Furthermore, the sum of the calculated $\Delta V_{D^+/D}^o$ and $\Delta V_{A^-/A}^o$ is negative, contrary to the sign obtained for ΔV_R . The difference between the calculated and the experimental values is beyond the experimental error and beyond an equivocal interpretation of the origin of the observed structural volume changes.

It has been already discussed that the theoretical prediction of the electrostriction caused by an ion in water is difficult because of the uncertainty in the type of interaction between the ion and the water molecules.^{34,35} The theoretical value of $B = 4.175 \text{ \AA}^{-1}$ in eq 11 estimated by assuming that the solvent is a continuum of dielectric constant ϵ does not quantitatively account for many of the effects observed in water, where specific interactions such as hydrogen bonding should be considered. Experimental results have shown that higher B values are needed to explain the partial molar volume of ions in water.³⁴ At 25 °C, various semiempirical equations yield B values ranging between 9.2 and 13.4 \AA^{-1} .³⁴

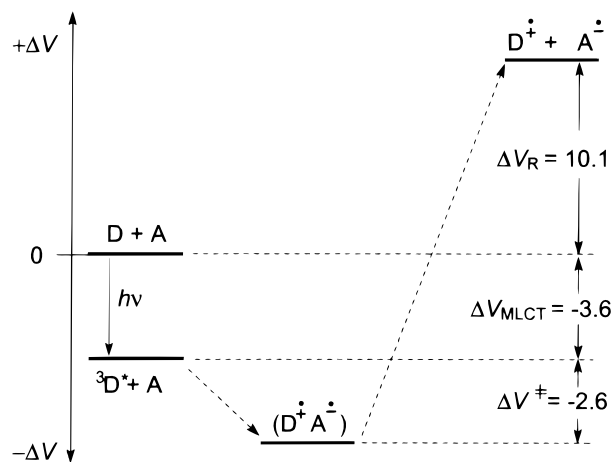
Another source of discrepancy may be the molecular shape and the effective radius of the ionic species used in eqs 11–13, especially for the MV²⁺ and MV⁺ cations. Ru(bpy)₃²⁺ and Ru(bpy)₃³⁺ are considered as rigid spheres with a similar radius of 4.8 Å calculated from crystallographic data.^{18,32} In this case, by using $B = 13.4 \text{ D}^{-1}$ and $r = 4.8 \text{ \AA}$, eq 12 yields $\Delta V_{D^+/D}^o = -14.0 \text{ cm}^3/\text{mol}$, in good agreement with the experimental value of $(-15.4 \pm 1.5) \text{ cm}^3/\text{mol}$.³

However, this straightforward approach is not possible for MV²⁺ and MV⁺ due to their nonspherical (rodlike) geometry and to the fact that the charges are not localized in the center of the species. The radius of 3.3 Å was estimated from CPK space-filling models, by using $r = [(d_x d_y d_z)^{1/3}]/2$.¹² The same authors obtained a value of $r = 7.0 \text{ \AA}$ for Ru(bpy)₃²⁺, by using the same calculation method. Then, it could be possible that the value of 3.3 Å for the MV²⁺ radius is also larger than the effective one, similar to the difference between the calculated and the crystallographic radius of Ru(bpy)₃²⁺ (vide supra).

Notwithstanding these difficulties, it is possible to roughly estimate a value of $\Delta V_{A^-/A}^o = +18.3 \text{ cm}^3/\text{mol}$, closer to the value derived from the LIOAS data $[(+25.5 \pm 2.7) \text{ cm}^3/\text{mol}]$, by using eq 13 with $B = 13.4 \text{ \AA}^{-1}$ and an approximate effective radius of 2.2 Å for MV²⁺ and MV⁺.³⁶

Thus, with the modified eq 11 the present results can be explained and, therefore, the structural volume changes observed

SCHEME 2: Volume Profile for the Photoinduced Quenching Reaction of the ³MLCT State of Ru(bpy)₃²⁺ (³[Ru^{III}(bpy)₃^{•-}]²⁺) by MV²⁺ in Water. $D = \text{Ru(bpy)}_3^{2+}$, $A = \text{MV}^{2+}$. The Volume Changes Refer to $D + A$. Units of Structural Volume Changes Are cm³/mol



upon the electron-transfer reaction can be assigned to solvent reorganization (including specific effects which are already included in the semiempirical value of B) around the ionic species. We have invoked a similar effect in water (also under the application of a larger B value in the Drude–Nernst equation) to explain the data obtained during the photoinduced proton ejection.³⁷

The apparent volume of activation for the quenching reaction B , $\Delta V^\ddagger = -2.6 \text{ cm}^3/\text{mol}$, was determined from the pressure dependence of the lifetime of Ru(bpy)₃²⁺ in the presence of MV²⁺.³⁸ With this value together with those determined in this work for the formation of the ³MLCT state of Ru(bpy)₃²⁺, ΔV_{MLCT} , and for the formation of the free radical ions Ru^{III}-(bpy)₃³⁺ and MV⁺, ΔV_R , it is possible to describe the complete volume profile for the present photoinduced reaction (Scheme 2).

Since the free energy for the reaction $\Delta G_R = 162 \text{ kJ/mol}$ is known from independent measurements,¹² the entropy change for the formation of the free ions in neat water (before recombination) $T\Delta S_R = 176 \text{ kJ/mol}$ is calculated as the difference between the enthalpy change calculated with LIOAS, $\Delta H_R = (338 \pm 20) \text{ kJ/mol}$, and ΔG_R .

This large entropy increment is necessarily associated with the (relatively large) solvent expansion due to the reduced ion–solvent attraction concomitant with the reaction (vide infra).

IV. Salt Effect: Evidence for an Enthalpy–Entropy Compensation. For the electron-transfer quenching reaction performed in 0.1 M solutions of various salts, the ΔH_R and ΔV_R values strongly depend on the salt (Table 4). ΔH_R vs ΔV_R for the various salts together with the data in neat water (all for the same quencher concentration) clearly shows a linear correlation except for the data with NaBr (Figure 6).

The linearity of this plot confirms the assumption that the salt effect is only due to environmental rearrangements and that the intrinsic changes are constant along the salt series. Leaving out the data for the NaBr solutions, a linear regression fit in accord with eq 14 yields a good linear correlation ($r = 0.994$) with $C = (140 \pm 25) \text{ kJ/mol}$ and $X = (14.4 \pm 0.8) \text{ kJ/cm}^3$.

$$\Delta H_R = C + X\Delta V_R \quad (14)$$

A possible explanation for the deviation of the data in 0.1 M NaBr is the ability of bulky halide ions (Br⁻ and I⁻) to form

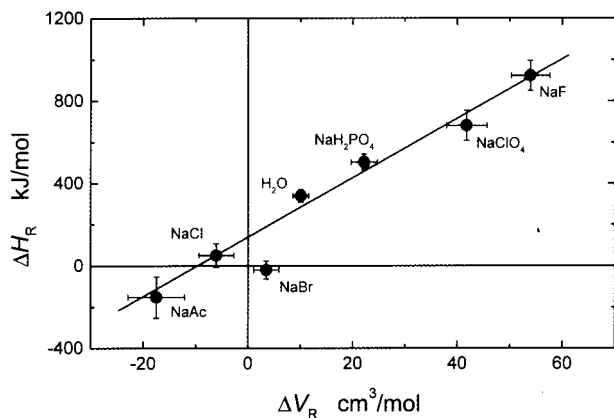


Figure 6. Structural heat evolved ΔH_R vs structural volume changes ΔV_R associated with the formation of the free radical ions $\text{Ru}(\text{bpy})_3^{3+}$ and MV^{+} in 0.1 M aqueous solutions of sodium salts (as indicated).

charge-transfer complexes with MV^{2+} in water.³⁹ In that case, both ΔH_R vs ΔV_R may contain a different intrinsic contribution than the rest of the data. The effect is not important for F^- and Cl^- due to the smaller size of these anions resulting in lower association constants.³⁹

By considering that the structural volume changes can be translated as entropy changes, as already reported,⁴ the intercept C should correspond to ΔG_R . It has been reported that $\Delta G_R = 162$ kJ/mol for the reaction is the same in 0.1 M solutions of the presently used salts as in water within the experimental error.¹² The linearity of the data in Figure 6 agrees with this fact and also the value of $C = (140 \pm 25)$ kJ/mol is coincident with that of ΔG_R within the experimental error. Thus, the following relationship 15 is readily written as

$$T\Delta S_R = \Delta H_R - \Delta G_R = X\Delta V_R \quad (15)$$

The linear dependency between ΔH_R and ΔV_R is the consequence of an enthalpy–entropy compensation effect induced by the added salt on the hydrogen-bond network structure of water, since ΔG_R remains constant throughout the salt series.¹²

The present slope value $X = (14.4 \pm 0.8)$ kJ/cm³ is very similar to the value (12 ± 1) kJ/cm³ observed for the linear regression data of the structural enthalpy and volume changes associated with the ³MLCT formation of the $\text{Ru}(\text{bpy})_2(\text{CN})_2$ and $\text{Ru}(\text{bpy})(\text{CN})_4^{2-}$ complexes in 0.1 M monovalent salts solutions. As mentioned in the Introduction, the ΔV_{str} values for these complexes in water were attributed to photoinduced changes in the hydrogen bond strength between the cyano ligands and the water molecules in the first solvation shell (specific solute–solvent interactions). The linear correlation between the structural enthalpy and volume changes in the aqueous salt solutions was interpreted as arising from an enthalpy–entropy compensation effect induced by the added salt on the hydrogen-bond network structure of water, which was sensed by the cyano complexes.⁴

Albeit the fact that with the cyano complexes the structural volume changes originated in specific hydrogen bond interactions, and in the present case the structural changes are due to effects based on changes in the ions charge number, the same mechanism seems to operate when salts perturbing the water network are added to the solutions (similar slopes values). In fact, taking into account the two sets of experiments, the average value of $X = (13 \pm 1)$ kJ/cm³ is equivalent to the $(c_p\rho/\beta)$ value at ca.30 °C for 0.1 M monovalent salt solutions, which is within the used temperature range and also is close to the temperature

(isokinetic temperature), at which the enthalpy–entropy compensation effect occurs in water.⁴⁰

The enthalpy–entropy effect arises when several molecular species are in dynamic equilibrium, and this equilibrium is perturbed by a particular factor, such as the addition of salts in the present case as well as in our previous study.^{4,41} The total decrease in an “attractive interaction” between the ions and water upon formation of $\text{Ru}^{\text{III}}(\text{bpy})_3^{3+}$ and MV^{+} ions “releases” water molecules to the bulk solution. Since water molecules have a strong tendency to participate as both hydrogen bond donors and acceptors, the formation of hydrogen bonds between the added salts and the water molecules should produce a decrease in enthalpy. In turn, hydrogen bonds require that the participating molecules become relatively fixed, therefore the entropy also decreases.

Inspired by the reported dependence¹² of the rate constant for quenching of $^3[\text{Ru}^{\text{III}}(\text{bpy})_3^{*}]^{2+}$ emission by the same anions as used in this work, and the free energy of hydration of those anions (ΔG_{hydr}^0),⁴² we searched for such type of correlation of the structural volume changes. ClO_4^- , Br^- , Cl^- , and CH_3CO_2^- follow a linear correlation between ΔV_R and ΔG_{hydr}^0 , whereas F^- and H_2PO_4^- do not fall into the linear correlation. The fact that such a dependence is not found with all anions indicates that while ΔG_{hydr}^0 controls the quenching within the solvent cage as demonstrated by Clark and Hoffman,¹² the total structural volume change ΔV_R (and therefore the entropy change) experienced upon formation of the radical ion pair (and before recombination) is determined by some additional factors. Since a cation and an anion radicals are produced, the ion pairing ability of $^3[\text{Ru}^{\text{III}}(\text{bpy})_3^{*}]^{2+}$ with the various added anions and the solvation of each radical might partially compensate, leading to deviations for some anions of the linear correlation between ΔV_R and ΔG_{hydr}^0 .

Acknowledgment. We thank Siggie Russell and Dagmar Lenk for their able technical assistance and Professor Kurt Schaffner for his continuous support. C.B. was supported in part by the EU grant INCO-ERBIC18CT960076.

References and Notes

- Braslavsky, S. E.; Heibel, G. E. *Chem. Rev.* **1992**, *92*, 1381–1410.
- (a) Feitelson, J.; Mauzerall, D. C. *J. Phys. Chem.* **1993**, *97*, 8410–8413. (b) Mauzerall, D.; Feitelson, J.; Prince, R. J. *J. Phys. Chem.* **1995**, *99*, 1090–1093. (c) Feitelson, J.; Mauzerall, D. C. *J. Phys. Chem.* **1996**, *100*, 7698–7703.
- Borsarelli, C. D.; Corti, H.; Goldfarb, D.; Braslavsky, S. E. *J. Phys. Chem. A* **1997**, *101*, 7718–7724.
- Borsarelli, C. D.; Braslavsky, S. E. *J. Phys. Chem. B* **1998**, *102*, 6231–6238.
- Habib Jiwan, J. L.; Wegewijs, B.; Indelli, M. T.; Scandola, F.; Braslavsky, S. E. *Recl. Trav. Chim. Pays-Bas* **1995**, *114*, 542–548.
- Drude, P.; Nernst, W. Z. *Phys. Chem.* **1884**, *15*, 79–85.
- (a) Patel, C. K.; Tam, A. C. *Rev. Mod. Phys.* **1981**, *53*, 517–550. (b) Tam, A. C. *Rev. Mod. Phys.* **1986**, *58*, 381–431.
- Rudzki, J. E.; Goodman, J. L.; Peters, K. S. *J. Am. Chem. Soc.* **1985**, *107*, 7849–7854.
- Weast, R. C. Ed. *CRC Handbook of Chemistry and Physics*, 67th ed.; CRC Press: Boca Raton, FL, 1986–87; pp F-4, F-5.
- Borsarelli, C. D.; Braslavsky, S. E. *J. Phys. Chem. B* **1997**, *101*, 6036–6042.
- Kalyanasundaram, K.; Kiwi, J.; Grätzel, M. *Helv. Chim. Acta* **1978**, *61*, 2720–2730.
- Clark, C. D.; Hoffman, M. Z. *J. Phys. Chem.* **1996**, *100*, 7526–7532.
- Juris, A.; Balzani, V.; Barigelletti, F.; Campagna, S.; Belser, P.; von Zelewsky, A. *Coord. Chem. Rev.* **1988**, *84*, 85–277 and references therein.
- Bolleta, F.; Juris, A.; Maestri, M.; Sandrini, D. *Inorg. Chim. Acta* **1980**, *44*, L175–L176.

- (15) Damrauer, N. H.; Cerullo, G.; Yeh, A.; Boussie, T. R.; Shank, C. V.; McCusker, J. K. *Science* **1997**, 275, 54–57.
- (16) van Houten, J.; Watts, R. J. *J. Am. Chem. Soc.* **1976**, 98, 4853–4858.
- (17) Kitamura, N.; Okano, S.; Tazuke, S. *Chem. Phys. Lett.* **1982**, 90, 13–16.
- (18) Yokoyama, H.; Shinozaki, K.; Hattori, S.; Miyazaki, F. *Bull. Chem. Soc. Jpn.* **1997**, 70, 2357–2367.
- (19) Goodman, J. L.; Herman, M. S. *Chem. Phys. Lett.* **1989**, 163, 417–420.
- (20) (a) Meyer, T. J. *Pure Appl. Chem.* **1986**, 58, 1193–1206 and references therein. (b) Yersin, H.; Humbs, W.; Strasser, J. *Coord. Chem. Rev.* **1997**, 159, 325–358.
- (21) Kober, E. M.; Sullivan, B. P.; Meyer, T. J. *Inorg. Chem.* **1984**, 23, 2098–2104.
- (22) (a) Whalley, E. *J. Chem. Phys.* **1963**, 38, 1400–1405. (b) Zimmt, M. B.; Vath, P. A. *Photochem. Photobiol.* **1997**, 65, 10–14.
- (23) Hamann, S. In *Modern Aspects of Electrochemistry*; Conway, B. E., Bockris, J. O. M., Eds.; Plenum Press: New York, 1974; Vol. 9, Chapter 2.
- (24) Bock, C. R.; Connor, J. A.; Gutierrez, A. R.; Meyer, T. J.; Whitten, D. G.; Sullivan, B. P.; Nagle, J. K. *J. Am. Chem. Soc.* **1979**, 101, 4815–4824.
- (25) Hips, K. W.; Crosby, G. A. *J. Am. Chem. Soc.* **1975**, 97, 7042–7048.
- (26) Norris, C. L.; Peters, K. S. *Biophys. J.* **1993**, 65, 1660–1665.
- (27) Hoffman, M. Z. *J. Phys. Chem.* **1988**, 92, 3458–3464.
- (28) Kalyanasundaram, K.; Neumann-Spallart, M. *Chem. Phys. Lett.* **1982**, 88, 7–12.
- (29) Chiorboli, C.; Indelli, M. T.; Rampi Scandola, M. A.; Scandola, F. *J. Phys. Chem.* **1988**, 92, 156–163.
- (30) Data obtained from the Supporting Information in reference.
- (31) Stranks, D. R. *Pure Appl. Chem.* **1974**, 38, 303–323.
- (32) Rillema, D. P.; Jones, D. S.; Levy, H. A. *J. C. S. Chem. Commun.* **1979**, 849–851.
- (33) Kosower, E. M.; Cotter, J. L. *J. Am. Chem. Soc.* **1964**, 86, 5524–5527.
- (34) Millero, F. J. *Chem. Rev.* **1971**, 71, 147–176.
- (35) Millero, F. J. In *Water and Aqueous Solutions*; Horne, R. A., Ed.; Wiley-Interscience: New York, 1972.
- (36) The value $r = 3.3 \text{ \AA}$ for MV^{2+} obtained by CPK space-filling models was corrected by the factor 4.8/7.0, which is the radius ratio between the crystallographic and CPK values for $\text{Ru}(\text{bpy})_3^{2+}$.
- (37) Borsarelli, C. D.; Braslavsky, S. E. *J. Photochem. Photobiol.* **1998**, 43, 222–228.
- (38) Kirk, A. D.; Porter, G. B. *J. Phys. Chem.* **1980**, 84, 2998–2999.
- (39) Bertolotti, S. G.; Cosa, J. J.; Gsponer, H. E.; Previtali, C. M. *Can. J. Chem.* **1987**, 65, 2425–2427.
- (40) The isokinetic temperature, T_{ik} is usually obtained as the slope of plots of $\delta\Delta H$ vs $T_{ik}\delta\Delta S$, where $\delta\Delta H$ and $\delta\Delta S$ correspond to the enthalpy and entropy variation upon condition change, for no change in free energy $\delta\Delta G = 0$. For many reactions in water T_{ik} ca. 300 K. For details see reference 47.
- (41) Grunwald, E. *Thermodynamics of Molecular Species*; Wiley: New York, 1996.
- (42) Marcus, Y. *Ion Solvation*; John Wiley: New York, 1985.